



Deposited via The University of Leeds.

White Rose Research Online URL for this paper:

<https://eprints.whiterose.ac.uk/id/eprint/217845/>

Version: Accepted Version

---

**Article:**

Zare, A., Bodisco, T.A., Verma, P. et al. (2022) Particulate number emissions during cold-start with diesel and biofuels: A special focus on particle size distribution. *Sustainable Energy Technologies and Assessments*, 51. 101953. ISSN: 2213-1388

<https://doi.org/10.1016/j.seta.2022.101953>

---

© 2022, Elsevier. This manuscript version is made available under the CC-BY-NC-ND 4.0 license <http://creativecommons.org/licenses/by-nc-nd/4.0/>. This is an author produced version of an article published in *Sustainable Energy Technologies and Assessments*. Uploaded in accordance with the publisher's self-archiving policy.

**Reuse**

This article is distributed under the terms of the Creative Commons Attribution-NonCommercial-NoDerivs (CC BY-NC-ND) licence. This licence only allows you to download this work and share it with others as long as you credit the authors, but you can't change the article in any way or use it commercially. More information and the full terms of the licence here: <https://creativecommons.org/licenses/>

**Takedown**

If you consider content in White Rose Research Online to be in breach of UK law, please notify us by emailing [eprints@whiterose.ac.uk](mailto:eprints@whiterose.ac.uk) including the URL of the record and the reason for the withdrawal request.

1 **Particulate number emissions during cold-start with diesel and biofuels: A special focus on**  
2 **particle size distribution**

3  
4 Ali Zare<sup>a,\*</sup>, Timothy A. Bodisco<sup>a</sup>, Puneet Verma<sup>b,c</sup>, Mohammad Jafari<sup>b,c</sup>, Meisam Babaie<sup>d</sup>,  
5 Liping Yang<sup>e</sup>, M.M Rahman<sup>f</sup>, Andrew P.W. Banks<sup>g</sup>, Zoran D. Ristovski<sup>b,c</sup>, Richard J. Brown<sup>b</sup>,  
6 Svetlana Stevanovic<sup>a</sup>

7  
8 <sup>a</sup> School of Engineering, Deakin University, VIC, 3216 Australia

9 <sup>b</sup> Biofuel Engine Research Facility, Queensland University of Technology (QUT), QLD, 4000 Australia

10 <sup>c</sup> International Laboratory for Air Quality and Health, Queensland University of Technology (QUT),  
11 QLD, 4000 Australia

12 <sup>d</sup> School of Computing, Science and Engineering (CSE), University of Salford, Salford, Manchester M5  
13 4WT, United Kingdom

14 <sup>e</sup> Institute of Power and Energy Engineering, Harbin Engineering University, No. 145-1, Nantong  
15 Street, Nangang District, Harbin, 150001, China

16 <sup>f</sup> School of Mechanical Aerospace and Automotive Engineering, Coventry University, Coventry CV1  
17 2JH, UK

18 <sup>g</sup> Queensland Alliance for Environmental Health Sciences, The University of Queensland, , QLD, 4072  
19 Australia

20  
21  
22 \*Corresponding author: Ali Zare, ali\_z4688@yahoo.com, ali.zare@deakin.edu.au

28 **Abstract**

29 The share of biofuels in the transportation sector is increasing. Previous studies revealed that  
30 the use of biofuels decreases the size of particles (which is linked to an increase in particulate  
31 toxicity). Current emission regulations do not consider small particles (sub-23 nm); however,  
32 there is a focus in future emissions regulations on small particles. These and the fact that  
33 within cold-start emissions are higher than during the warmed-up operation highlight the  
34 importance of a research that studies particulate matter emissions during cold-start. This  
35 research investigates the influence of biofuel on PN and PM concentration, size distribution,  
36 median diameter and cumulative share at different size ranges (including sub-23 nm and  
37 nucleation mode) during cold-start and warm-up operations using diesel and 10, 15 and 20%  
38 mixture (coconut biofuel blended with diesel). During cold-start, between 19 to 29% of total  
39 PN and less than 0.8% of total PM were related to the nucleation mode (sub-50 nm). Out of  
40 that, the share of sub-23 nm was up to 9% for PN while less than 0.02% for PM. By using  
41 biofuel, PN increased between 27 to 57% at cold-start; while, the increase was between 4 to  
42 19% during hot-operation. The median diameter also decreased at cold-start and the  
43 nucleation mode particles (including sub-23 nm particles) significantly increased. This is an  
44 important observation because using biofuel can have a more adverse impact within cold-  
45 start period which is inevitable in most vehicles' daily driving schedules.

46

47 **Keywords:** Particle size distribution; PN; sub-23 nm; biofuel; cold-start.

48

49 **Word count:** 7338

---

**Abbreviations**

---

NOx	Nitrogen oxides
CO	Carbon Monoxide
HC	Hydrocarbon
PM	Particle mass
PN	Particle number
BSFC	Brake Specific Fuel Consumption
CMD	Count median diameter
ECU	Engine control unit
EU	European Union
VOCs	Volatile organic compounds

---

50

51

52 Highlights

- 53 1. This study investigated engine-out particle emissions and size distribution
- 54 2. Cold-start, hot-start, and two intermediate warm-up phases were studied
- 55 3. Nucleation mode particles increased as the engine warmed up
- 56 4. During cold-start, using biofuel decreased the size of particles
- 57 5. Sub-23 nm fraction contributed up to 0.02% and 9% to cumulative PM and PN

58

59

60

61

## 62 1. Introduction

63 The transportation sector has been undergoing a significant transformation with the  
64 utilisation of different strategies and technologies to reduce harmful emissions [1]. One of  
65 these strategies is related to fuel. The adverse effect of using fossil fuels in the transportation  
66 sector has created significant interest in renewable alternatives, such as biofuels. There have  
67 been incentives in place to increase the share of such renewable alternatives. For example,  
68 EC Directive 2003/30 was issued to increase the share of biofuel to 5.75% by 2010 and  
69 Directive 2009/28/EC targeted a share increase to 10% by 2020. One of the reasons for  
70 increasing the share of renewable fuel in the transportation sector can be the advantages it  
71 has on engine performance and exhaust emissions [2-4].

72 In terms of engine performance parameters, it has been reported that using biofuels (such as  
73 jatropha biodiesel) can improve the thermal efficiency of diesel engines when compared to  
74 diesel fuel; however, it depends on the type of biofuel [5-7]. Friction parameters were also  
75 reported to be lower with biodiesel owing to their better lubricity [8, 9]. However, fuel  
76 consumption parameters such as brake specific fuel consumption (BSFC) were reported to be  
77 higher and the engine power was reported to be lower with biofuel derived blends [10, 11].  
78 The higher viscosity, higher density and lower calorific values of biofuels were reported to be  
79 primary reasons. In terms of emissions, lower hydrocarbon (HC) and carbon monoxide (CO)  
80 emissions were reported to be advantages of using biofuels [12-14]. However, it has been  
81 frequently reported that nitrogen oxides (NOx) emissions increase with biofuels (some  
82 articles claimed otherwise) [15-17]. Maybe the most highlighted advantage of using biofuel is  
83 the decrease in particulate matter emissions; however, some articles reported a different  
84 observation [18, 19]. It has been frequently reported that particulate matter emissions  
85 decrease significantly due to the oxygen content of the biofuel [18, 20, 21].

86 Particulate matter emissions can adversely affect our environment and are identified as a  
87 global risk factor as these emissions have been reported to be associated with  
88 cardiorespiratory health problems [22-24]. It was shown that prolonged exposure to  
89 particulate matter emissions is associated with an increase in free-radicals which adversely  
90 impact health [25-27]. Particulate matter emissions can be evaluated from two inter-  
91 correlated perspectives. The first aspect is the particulate mass (PM) which reports the mass  
92 of particles. However, this measurement might not be able to provide sufficient information  
93 when it comes to the health hazards from particles, as those very small particles which are  
94 harmful have a lower contribution to PM [28]. However, the second perspective, particulate  
95 number (PN), is more informative and has gained a lot of attention, therefore it became  
96 mandated in the recent emissions regulations [29]. For passenger cars, reporting PN  
97 emissions became mandated from the Euro 5 emissions regulation [29], while there was no  
98 regulation on PN in Euro 1-4 [29]. The PN, which is the count of individual particles can include  
99 small particles even those with nearly zero weight and contribution to PM.

100 Using biofuel has been reported to have different effects on PN emissions, some reported  
101 higher PN with biofuels and some reported lower [18, 30]. However, most of the reports in  
102 the literature showed that using biofuel decreases the size of particles [31, 32]. This is  
103 important as it has been reported that a decrease in particle size is associated with an increase  
104 in toxicity [33]. However, in the most recent emission regulations such as Euro 5 and 6 and  
105 WLTP (worldwide harmonised light vehicles test procedure), there is a guideline for PN  
106 measurement—PMP (particle measuring method)—which does not consider sub-23 nm  
107 particles [34-36]. PMP does specify the count efficiency of 50% ( $D_{50}$ ) at 23 nm and 90% ( $D_{90}$ )  
108 at 41 nm, and it has been reported in the literature that decreasing  $D_{50}$  from 23 nm to smaller  
109 sizes such as 10 nm can significantly increase the PN emissions from vehicles [37, 38]. For

110 example, Leach et al. [38] reported that decreasing  $D_{50}$  and  $D_{90}$  to 10 nm and 23 nm leads to  
111 36% higher PN. This and the increasing share of biofuel in the transportation sector highlight  
112 the importance of studying PN emissions in more detail such as looking into the size of  
113 particles.

114 PN emissions from an engine depend on different factors such as operating conditions [39].  
115 For a high portion of vehicles, the cold-start operation is a norm which occurs mostly in the  
116 morning and afternoon when people start their vehicle after some hours of engine-off and  
117 drive between home and work. It has been reported that a significant number of trips  
118 between home and work start and finish during the cold-start period [40]. For example, a  
119 study of more than one thousand trips showed that more than 30% of the trips started and  
120 finished within the cold-start period [41]. Regulation (EU Directive 2012/46/EU) considers the  
121 cold-start period from engine start—after 12 hours soak (or 6 hours forced cooled)—either  
122 for the first 5 minutes or during the time that the temperature of engine coolant increases to  
123 70°C. Within this period, the engine temperature is sub-optimal affecting the combustion  
124 process [42]. Consequently, engine emissions and performance are different in comparison  
125 with hot-operation [43-45]. For example, fuel consumption and friction power were reported  
126 to be higher when the engine is cold [46]. This was reported to be because of the high viscosity  
127 of the engine oil at lower temperatures, which consequently leads to higher friction, therefore  
128 more fuel needs to be burnt to maintain power [40, 46]. Fuel evaporation and atomisation  
129 are also impacted by the lower temperature of the engine and fuel during cold-start which  
130 also impacts emission and performance parameters [18].

131 It has been reported that during cold-start, emissions are higher than when the engine is fully  
132 warmed up [47, 48]. For example, a study used a custom driving cycle and showed that during

133 the cold-start period of the cycle, PN emissions with biofuel increased significantly compared  
134 to the hot-operation period [47]. Another study showed that around one-third of the emitted  
135 PM emissions were related to the first 12% of the total distance (Phase 1) of the LA92 Unified  
136 Driving Cycle [49]. It also reported that compared to Phase 3 of that cycle, in which the engine  
137 was fully warmed up, during Phase 1, which was cold-start, the PM emissions were 7.5 times  
138 higher. Some studies in the literature investigated other emissions such as CO, CO<sub>2</sub> and NO<sub>x</sub>  
139 [40, 50, 51]. However, there are a few studies that investigated PN emissions and size  
140 distribution during cold-start in detail, when compared to other emissions [52]. Also, most of  
141 the cold-start experimental studies in the literature used driving cycles such as NEDC (New  
142 European Driving Cycle) or WLTC (worldwide harmonised light vehicles test cycle) which has  
143 abrupt load/speed changes. The results of such studies were shown with the averaged value.  
144 However, it is essential to study the influence of transient engine temperature while the  
145 engine is warming up on exhaust emissions such as PN. It will be seen in this current study  
146 that cold-start and engine warm-up have different stages and therefore different impacts on  
147 exhaust emissions.

148 This research aims to study the influence of fuel and transient engine temperature at different  
149 stages of engine warm-up (including cold-start) on particulate matter emissions from  
150 different aspects including PN, PN and PM size distribution and median diameter, the share  
151 of particles at different sizes, nucleation mode particles and sub-23 nm particles. The  
152 increasing share of biofuels in the market, with the inherent decrease in particle size and the  
153 associated increase in toxicity, increased emissions during cold-start coupled to future  
154 emissions regulations on small particles, and the fact that the current emission regulations do  
155 not consider sub-23 nm particles, all highlight the importance of this study. By using and  
156 comparing different biofuel blending ratios (10, 15 and 20%), this study can be helpful to

157 engine researchers when it comes to nucleation mode and sub-23 nm particles the upcoming  
158 emissions regulations.

## 159 **2. Methodology**

160 The engine used in this study was a Cummins ISBe220 diesel engine (designed and  
161 manufactured by an American company) which is an in-line 6-cylinder, turbocharged,  
162 common-rail engine, as shown in Table 1. The maximum torque and power with this engine  
163 are 820 Nm (at 1500 rpm) and 162 kW (at 2500 rpm) and the engine was coupled to an in-  
164 house hydraulic dynamometer (electronically-controlled). The experiments were done at  
165 QUT Biofuel Engine Research Facility (BERF) in Brisbane, Australia.

166

167 Table 1 Engine specifications

<b>Model</b>	<b>Cummins ISBe220 31</b>
Aspiration	Turbocharged
Fuel injection	Common rail
Cylinders	6 in-line
Capacity	5.9 L
Bore × stroke	102 × 120 (mm)
Maximum torque	820 @ 1500 (Nm @ rpm)
Maximum power	162 @ 2500 (kW @ rpm)
Compression ratio	17.3:1

168

169 Figure 1 shows a schematic diagram of the experiment setup. Engine and dynamometer data  
170 were collected with Dynolog software. The in-cylinder data such as crank angle and injection  
171 signals were collected using a Kistler (6053CC60) transducer, Kistler type 2614 sensor and  
172 DT9832 A-to-D convertor, which all were connected to an in-house National Instruments

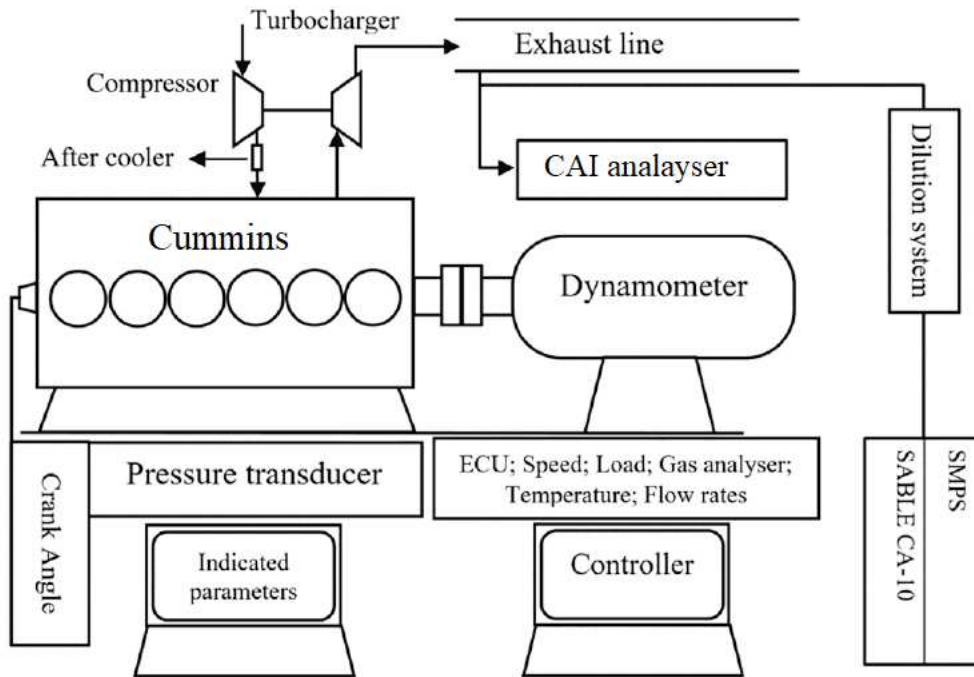
173 LabView program [53, 54]. The accuracy of the measuring instruments are shown in Appendix  
174 (Table A1).

175 To better evaluate the pure effect of fuel properties and also the engine temperature, this  
176 study evaluated the engine-out emissions instead of tailpipe emissions (which are sampled  
177 before any after-treatment system). This way the emissions do not depend on the after-  
178 treatment systems performance/type. Therefore, the fundamental study will not be limited  
179 and results can give more information about the real engine dependent emission [55]. In  
180 order to measure particulate matter emissions (such as particle number, mass, size  
181 distribution), this study used a TSI scanning mobility particle sizer (SMPS) consisting of a TSI  
182 3071A classifier (which preselects the particles in different sizes) and a TSI 3782 CPC (which  
183 grows the particles to make them detectable for the optic). SMPS is designed and  
184 manufactured by TSI which is an American company. SMPS has a size resolution capability of  
185 128 channels per decade, which results in 192 channels in total. The exhaust gas (which had  
186 a temperature of  $\sim 350$  °C) was directed to the SMPS, but after being diluted ( $\sim 20$  times) with  
187 ambient air ( $\sim 23$  °C) which was passed through a HEPA filter in a constant volume dilution  
188 system (CVS). The CVS setup was followed by the European legislation (Commission  
189 Regulation (EU) 2017/2400). To calculate the dilution ratio, a CAI-600 and a SABLE CA-10 CO<sub>2</sub>  
190 analysers (designed and manufactured by American companies) were used before and after  
191 the dilution system measuring the CO<sub>2</sub> emissions.

192 The exhaust particles are made of solid particles, volatiles and liquid droplets. Usually, the  
193 PMP method uses a volatile particle remover (VPR) system including three stages of hot  
194 dilution (PND<sub>1</sub>), heated evaporative tube (ET) and cold dilution (PND<sub>2</sub>) to minimise the effect  
195 of volatiles and liquid droplets ensuring that the particle counter measures solid particles

196 (ECE/TRANS/WP.29/GRPE/2016/3 amended by GRPE-72-09-Rev.2) [56]. Regarding the  
197 difficulty of sub-23 nm measurement with current instruments in the market [36], it is worth  
198 mentioning that SMPS is capable to measure particles above 10 nm including solid particles  
199 and volatiles.

200 This study reports PN and PM, and also PN and PM size distribution. Regarding the PN and  
201 PM size distribution, SMPS measures the number of concentration in a given channel ( $dN$ )  
202 and divides it by the geometric width of the size of channel, and reports the normalised  
203 number concentration ( $dN/d\log D_p$ ), where  $D_p$  is the geometric midpoint of the particle size  
204 channel. The conversion of PN to PM was done through the Aerosol Instrument Manager  
205 Software for SMPS Spectrometer using the formula  $dM = dN \cdot (\pi/6) D_p^3 \rho$ , where  $\rho$  is density,  
206 and reporting the normalised mass concentration using the formula  $dM/d\log D_p = dN/d\log D_p$   
207  $\cdot (\pi/6) D_p^3 \rho$  [57]. In general, based on the size distribution, the measured ultrafine particles  
208 can be classified into two modes; nucleation mode and accumulation mode [28]. The  
209 nucleation mode particles are defined as particles with diameters less than 50 nm, and the  
210 size of accumulation mode particles is between 50-500 nanometres, and these definitions are  
211 used in this study to better interpret the data [28].



212

213

Figure 1 Test setup schematic diagram

214

215 Given that this study intended to investigate particulate matter emissions based on the  
 216 current and future emissions regulation requirements, the selection of the fuels was  
 217 conducted in a way to cover past, current and future biofuel blending ratio in the market.  
 218 Therefore, it used diesel, and then made three diesel/biofuel blends of 10, 15 and 20% (by  
 219 volume) denoted as D90C10, D85C15 and D80C20 using coconut oil biofuel (this study is a  
 220 part of a project which investigates the potential of using different biofuels in diesel engines  
 221 in Marshal Islands which have a high resource of coconut). In the tested fuel names, D stands  
 222 of diesel and the digits after that show the volume of diesel in the blend. And C stands for  
 223 coconut biofuel and the two digits after C shows the blending ratio. These fuel blends will be  
 224 evaluated against diesel (D100).

225 Table 2 shows the tested fuel properties and Table 3 shows the chemical composition of fuels  
 226 analysed by a GC/MS instrument (Trace 1310 Gas chromatograph, model ISQ, single

227 quadrupole MS). Diesel (D100) contained aromatic compounds (benzene and its derivatives,  
 228 naphthalene, xylene, phthalan, mesitylene) and aliphatic compounds (mainly alkanes with 7-  
 229 13 carbons, low concentrations of limonene). D90C10, D85C15, and D80C20 also contained  
 230 cycloalkanes, cyclohexane and cyclooctane. With D100, the aromatic content was higher  
 231 compared to other fuels. Compared to neat diesel, fuels with a lower blending ratio do not  
 232 change the fuel properties significantly. For example, the density of the tested fuels, D100,  
 233 D90C10, D85C15 and D80C20 were 0.84, 0.843, 0.845 and 0.846 g/cc. Also, the lower heating  
 234 value of the tested fuels, D100, D90C10, D85C15 and D80C20 were 41.77, 41.31, 41.09 and  
 235 40.86 MJ/kg, respectively. However, even small changes in fuel properties can affect engine  
 236 performance and emissions. For example, the higher density and lower calorific value of  
 237 biofuel blends can negatively impact engine power and also fuel consumption parameters  
 238 such as BSFC [8]. The fuel oxygen content of biofuel is another property that distinguishes  
 239 biofuel from diesel (which has no oxygen content). It has been frequently reported that fuel  
 240 oxygen content is the primary driver for decreased PM emissions with biofuels [18, 19, 58].

241

242 Table 2 Fuel properties

	D100	C100	D90C10	D85C15	D80C20
Density at 15 °C (g/cc)	0.84	0.87	0.84	0.84	0.85
Kinematic viscosity at 40 °C (mm <sup>2</sup> /s)	2.64	4.82	2.86	2.97	3.08
Cetane number	53.30	58.60	53.83	54.10	54.36
Lower heating value (MJ/kg)	41.77	37.20	41.31	41.08	40.86
Higher heating value (MJ/kg)	44.79	39.90	44.30	44.06	43.81

243

244

245 Table 3 Fuel analysis using GC/MS (Model ISQ, single quadrupole MS, Trace 1310 Gas  
 246 chromatograph).

	Area %				
	aromatic	aliphatic	cyclic hydrocarbons	hydrazide	oxygenated hydrocarbons
D90C10	0.0879-0.169	0.0866-0.367	0.119-1.12	1.09-2.62	0.192-0.305
D80C20	0.0433-0.0968	0.0398-0.741	0.0394-0.222		0.0416-0.076
D100	1.43-5.66	1-12.24			

247

248 The fuels used in this study were tested under constant load (25%) and speed (1500 rpm).

249 The rationale for using a constant load and speed was to facilitate the fundamental

250 investigation into the influence of fuel type & engine temperature under cold-start and during

251 engine warm-up. Most of the studies on cold-start in the literature used a drive cycle such as

252 NEDC or WLTC and compared the first part of the cycle with the rest and made the conclusion

253 about cold-start contribution. However, these driving cycles consist of frequent load and

254 speed changes which add more variables to the analysis, complicating and limiting the

255 investigation about the pure influence of fuel type and engine temperature on emissions

256 within cold-start period. Therefore, this experimental investigation used a constant speed and

257 engine load to limit the number of influential factors that can potentially aid a better

258 judgment on the effects of engine temperature and fuel properties.

259 Experiments were done every morning with at least 12-hours of engine-off period at the

260 ambient temperature on consecutive days in an engine laboratory. Before starting each test,

261 coolant temperature and lubricating oil temperature were checked to be the same as ambient

262 temperature, as per the regulation (EU Directive 2012/46/EU). Given that the engine room

263 had an air-conditioning system, the ambient temperature during the test stayed constant

264 (23±5 °C). For each test, the engine was started and ran under a quarter load (25%) at the

265 speed of 1500 rpm for more than 30 min to stabilise. The statistical analysis of the test  
266 repeatability is shown in Appendix.

267 In diesel engines, the formation of particulate matter emissions depends on a number of  
268 variables such as engine operating condition and fuel properties [18]. During cold-start  
269 operation, the engine temperature and fuel properties are significantly influential factors.  
270 Figure 2 shows how the engine coolant temperature increases during cold-start operation  
271 with the tested engine for one of the tests. According to the regulation, (EU Directive  
272 2012/46/EU), the cold-start period is defined from when the engine starts after 12 hours soak  
273 (or 6 hours forced cooled soak) at the ambient condition either for the first 5 minutes or  
274 during the time that the temperature of engine coolant increases to 70°C. However, after this  
275 period, the coolant temperature still has an increasing trend indicating the sub-optimal  
276 engine temperature (Figure 2). Also, it can be seen that there is a lag between the engine  
277 lubricating oil temperature and coolant temperature. Compared to the coolant temperature,  
278 the engine lubricating oil temperature remains sub-optimal for a longer period). The sub-  
279 optimal temperature period outside the formal cold-start boundaries can affect the engine  
280 performance and exhaust emissions [59, 60]. Figure 2 also shows that for the tested engine,  
281 even within the formal cold-start period, when the engine temperature reaches to 65°C, the  
282 start of injection is changed by the injection strategy commanded by the ECU of the tested  
283 engine, and this injection strategy change affects the exhaust emissions and engine  
284 performance parameters. It is worth mentioning that while the start of injection changed, the  
285 injection period (therefore, the injection mass) remained constant, as the injection was  
286 controlled by the ECU and, the injection period was independent of the start of injection. Also,  
287 there was no modification to the engine ECU/calibration for different fuel blends. Therefore  
288 the start of injection timing stayed the same for all the tests.

289 As discussed, it can be seen that from the engine start until the stable operation, there are  
290 some periods with different characteristics and variables. Therefore, in order to better  
291 analyse the influence of fuel properties and engine temperature, this research divides the  
292 engine warm-up period into four phases to minimise the number of variables in each phase.

293 • Phase 1: Formal engine cold-start, constant start of injection, coolant and oil  
294 temperatures are less than 65°C.

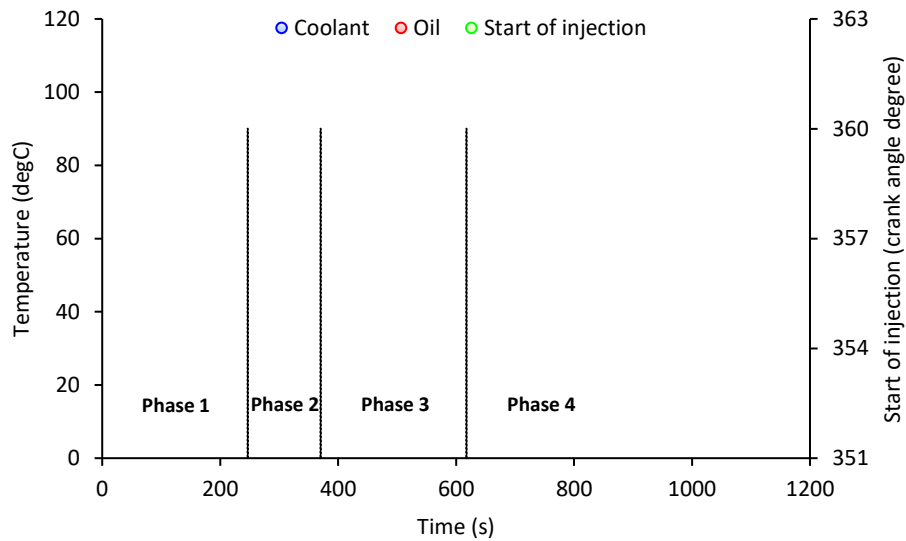
295 • Phase 2: Start of injection is increasing, coolant and oil temperatures above 65°C and  
296 still increasing.

297 • Phase 3: Constant start of injection, optimal coolant temperature, sub-optimal oil  
298 temperatures.

299 • Phase 4: Engine hot-operation, start of injection is constant, coolant and oil  
300 temperatures are optimal.

301 This study used an SMPS analyser with a 2 min sampling time. The first two samples were  
302 measured within Phase 1, the third sample was measured in Phase 2, the fourth and fifth  
303 samples fell into Phase 3, and the last two samples were measured within Phase 4.

304



305

306 Figure 2 Engine coolant temperature, engine oil temperature and start of injection during the test  
307 with diesel

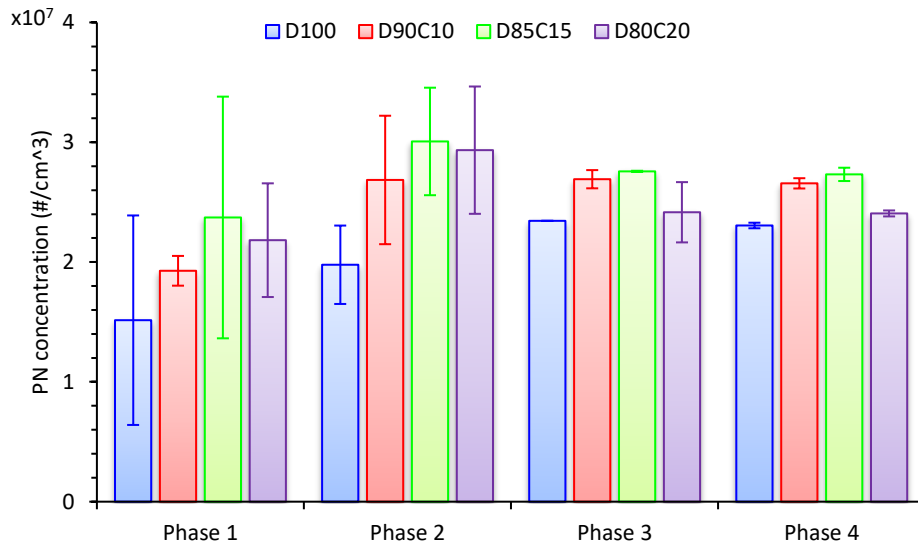
308

### 309 3. Result and discussion

310 This section analyses the PN concentration and evaluates the particle number and mass size  
311 distribution. It also investigates the median diameter and the share of PN and PM at different  
312 sizes including accumulation mode, nucleation mode and sub-23 nm particles.

313 Figure 3 presents the PN concentration at the four different phases. It shows that for each  
314 fuel the PN concentration in Phase 1 was lower than the other phases. Given that the engine  
315 load and speed were constant within all phases, the engine temperature can be identified as  
316 an influential factor, as shown in the literature [61]. Looking at each phase, it can be seen that  
317 the use of biofuel increased PN emissions in all of the phases. This expected result shows that  
318 fuel properties are influential, as reported before in the literature [62, 63].

319



320

321

Figure 3 PN concentration at different phases with all the tested fuels

322

323

When it comes to the potential health impact of particles, PN can also be analysed in more

324

detail by looking into the size distribution of particles [28, 33]. Reported hypotheses

325

mentioned that when compared to bigger particles, small particles penetrate in lungs deeper

326

and their relatively larger surface area increases the reaction with lung cells; a decrease in the

327

size of particles is also associated with an increase in toxicity [33]. Figure 4 shows the median

328

diameter of the particles with all the tested fuels at different phases. It can be seen that the

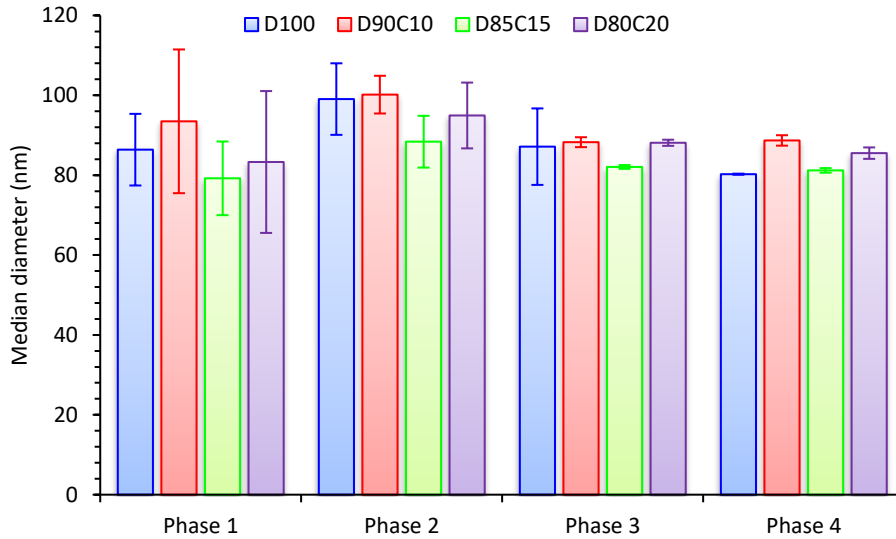
329

size of the particles changes as the engine warms up. From Phase 2 to Phase 4, it can be seen

330

that as the engine warms up, the size of particles slightly decreases [64].

331



332

333

Figure 4 PN median diameter at different phases with all the tested fuels

334

335 As discussed, cold-start operation and fuel properties are two factors that can significantly  
 336 affect the PN concentration and particle size, shown in the literature as well [47]. Therefore,  
 337 the following analysis is divided into two parts. It first analyses the data from the engine  
 338 temperature and cold-start perspective and then discusses the influence of fuel properties.

### 339 3.1 Influence of engine temperature

340 Figure 5 shows the variation of PN concentration at the different phases as compared to Phase  
 341 1 (cold-start). It can be seen that the PN concentration was higher at other phases when  
 342 compared to Phase 1. As a constant engine load/speed was maintained through all of the  
 343 phases, the engine temperature can be considered as the driving factor for any change [52].  
 344 In Figure 5, the exhaust temperature is used as an indicator of the engine temperature at the  
 345 different phases. It can be seen that the exhaust temperature increased from Phase 1 to  
 346 Phase 4, however, the change between Phases 3 and 4 was not as significant as between  
 347 Phases 1 and 2. The reason for using the exhaust temperature as an indicator instead of

348 coolant temperature, was that when the coolant temperature reaches to an optimum level,  
349 the engine is still warming up.

350 Phase 1, which had the lowest PN, falls into the cold-start period. As per the regulation, EU  
351 Directive 2012/46/EU, the cold-start period can last 5 min from the engine start or until the  
352 engine coolant temperature reaches 70°C. During Phase 1, the engine coolant temperature  
353 was less than 70°C. Also, during this phase, the start of injection did not change as the engine  
354 coolant temperature was less than 65°C, which is the threshold for the injection strategy of  
355 the tested Cummins engine.

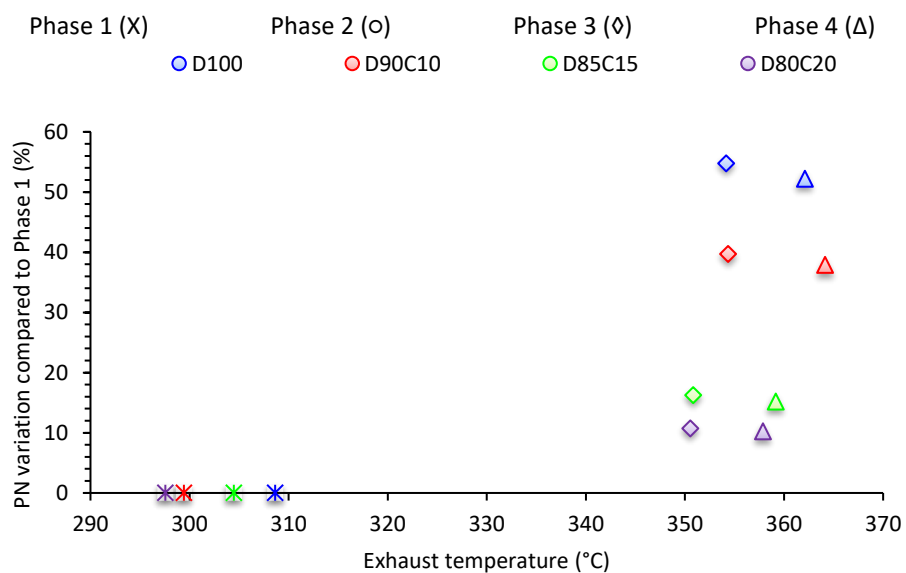
356 During Phase 2, the PN concentration was significantly higher than Phase 1. This increase was  
357 between 27 to 39%. For example, with neat diesel, D100, the PN concentration increased by  
358 31%, with D80C20 the PN concentration increased by 39%. The significant change between  
359 Phases 1 and 2 is a combination of the increase in engine temperature and the injection  
360 strategy change, with the latter being assumed as the dominant driver. During this unsteady  
361 phase, coolant temperature increased to 65°C and the start of injection changed significantly  
362 as by the ECU. This significant increase in the start of injection can be seen in Figure 2. Phase  
363 2 cannot be considered as cold-start because the engine temperature within this phase  
364 increased to higher than 70°C. In this phase, both the engine coolant and oil temperatures  
365 were sub-optimal and still increasing.

366 Phase 3 had higher PN compared to Phase 1. The increase was between 11 to 55% with  
367 different fuels. For example, with D80C20, the PN concentration increased by 11%, with D100,  
368 PN increased by 55%. Within this phase, the engine coolant temperature was optimal.  
369 However, this phase cannot be considered as hot-operation (stable operation) given that  
370 within this phase the engine oil temperature was sub-optimal and still increasing. Comparing

371 this to Phase 2, within this phase, the start of injection stayed constant and did not change  
372 until the end of the test.

373 Phase 4 can be considered as hot-operation given that within this phase, the engine  
374 load/speed and the start of injection stayed constant, and also the engine oil and coolant  
375 temperatures were optimal. Phase 4 shows that the PN concentration during this hot-  
376 operation phase was higher than cold-start (Phase 1). The range of increase with different  
377 fuels was from 10 to 52%. For example, with D100, the PN concentration was 52% higher than  
378 Phase 1, with D80C20, the PN concentration was 11% higher. It can also be seen that, for all  
379 of the fuels, the PN concentration in Phase 3 is slightly higher than Phase 4 (~2%). The  
380 difference between Phase 3 and Phase 4 shows the effect of sub-optimal oil temperature  
381 when the coolant temperature is optimal.

382

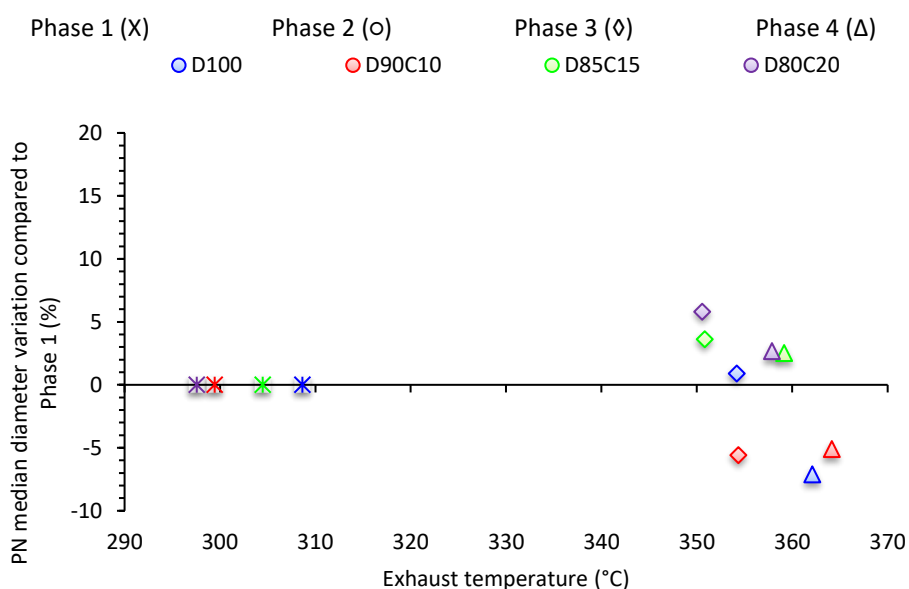


383

384 Figure 5 PN variation compared to Phase 1 vs. exhaust gas temperature at different phases with all  
385 the tested fuels

386 The main contributors to PN emissions are nanoparticles [28]. Figure 6 shows that for each  
 387 fuel, compared to Phase 1, the median diameter increased significantly in Phase 2 and then  
 388 decreased in Phases 3 and 4. It is reported in the literature that increased exhaust gas  
 389 temperature is associated with an increase in nanoparticles [65]. This can be seen in Figure 7,  
 390 where for each fuel from Phase 2 to Phase 4 the increased exhaust temperature is associated  
 391 with a decreased median diameter. This can also be seen in Figure 7 where moving from Phase  
 392 2 to Phase 4 is associated with an increased number of nanoparticles.

393



394

395 Figure 6 Median diameter variation compared to Phase 1 vs. exhaust gas temperature at different  
 396 phases with all the tested fuels

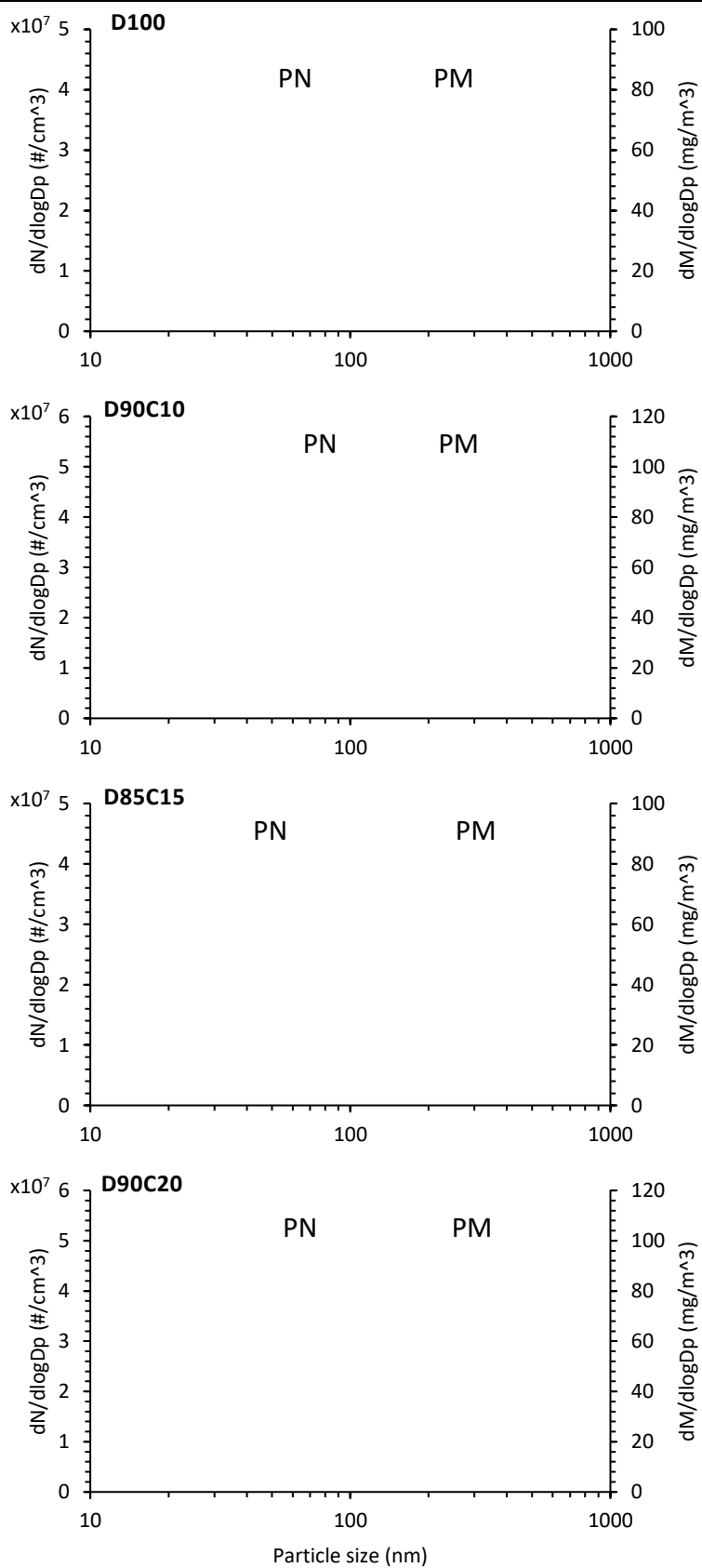
397

398 Figure 7 shows the PN and PM size distribution at the four phases of engine warm-up. In this  
 399 study, particles are categorised into nucleation (5-50 nm) or accumulation modes (50-500 nm)  
 400 [28]. Nucleation mode particles, which contribute negligibly to PM, but significantly to PN, are  
 401 predominately volatile organic compounds (VOCs) and sulfur compounds—formed within

402 dilution and sampling—and also metal compounds and solid carbons—formed during the  
403 combustion process [28]. In Figure 7, comparing the PN and PM size distribution graphs for  
404 each fuel at each phase, which are shown with the same colour but two different shapes (o  
405 and Δ) in each sub-figure, shows that for the size range of 5 to 50 nm in which the number of  
406 particles was significantly high, the mass of particles was low. This can be better observed in  
407 Figure 8 where the cumulative share of PN and PM at different size ranges is presented. As  
408 can be seen, for all of the fuels at all the phases, the cumulative share of sub-50 nm particles  
409 was between 0.3 to 0.9% of the total mass, while depending on the phase/fuel 11 to 29% of  
410 the total PN were related to sub-50 nm. Also, depending on phase/fuel, for the sub-30 and  
411 sub-23 nm particles, the PM cumulative share were up to 0.06 and 0.02%; while, their  
412 cumulative PN share were 13 and 9%, respectively. Therefore, excluding sub-23 nm particles  
413 in the current regulation means neglecting a significantly high number of small and toxic  
414 particles, considering the number of vehicles in cities and the PN limit in the emissions  
415 standards (e.g.  $6 \times 10^{11}$  #/km in Euro 6 and WLTP).

416

○ Phase 1   ● Phase 2   ● Phase 3   ● Phase 4



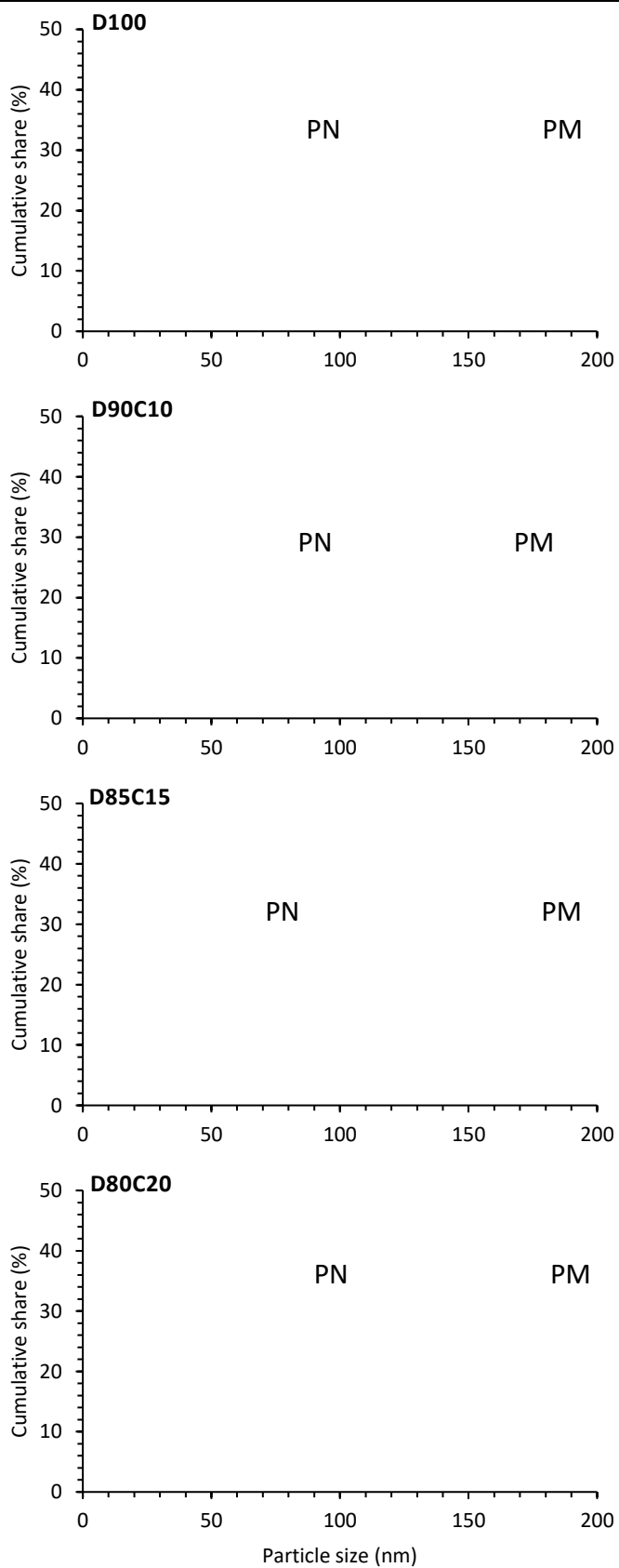
417

Figure 7 PN and PM size distribution at different phases with all the tested fuels

418 The main contributor to the accumulation mode particles are carbonaceous agglomerates  
419 and adsorb materials [28]. The agglomeration of particles in the nucleation mode by the  
420 condensation of volatile materials can also form some particles in the accumulation mode  
421 [28]. Figure 8 shows that sub-100 nm particles contributed to 53-67% of PN while only to 8-  
422 14% of PM. 92-96% of PN was related to sub-200 nm, while only 50-66% of the total mass was  
423 related to these particles. It can be seen that in the accumulation mode, the share of PN  
424 decreased as the share of PM increased. Comparing PN and PM size distribution graphs in  
425 Figure 7 shows that the contribution of particles above 50 nm to PM was significant. This is  
426 more significant for the sizes above 100 nm where the share of PN was decreasing. This can  
427 be better explained by comparing Figure 9, which shows the PM median diameter, with Figure  
428 4, which shows the PN median diameter. It can be seen that the PM median diameter was  
429 between 173 to 213 nm, while for PN the median diameter changed between 79 to 100 nm.  
430 This can clearly show that accumulation particles have a major contribution to PM. The PN  
431 and PM size distribution in each phase are different and need to be further investigated.

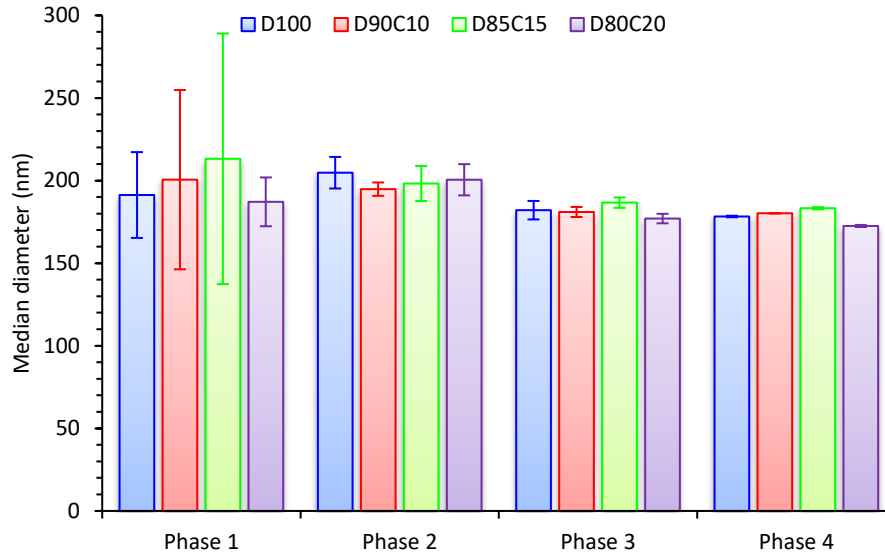
432

○ Phase 1   ● Phase 2   ● Phase 3   ● Phase 4



433

Figure 8 Cumulative PN and PM share at different phases with all of the tested fuels



434

435 Figure 9 PM median diameter at different phases with all of the tested fuels

436

437 A decrease in the size of particles can indicate a higher share of nucleation mode. The median  
 438 diameter trend observed in Figure 4 reflects the trend of PN share in the nucleation mode in  
 439 Figure 8. The median diameter of the particles increases from Phase 1 to Phase 2 (because of  
 440 the change in injection strategy) and decreases gradually through the engine warm-up period.  
 441 Therefore, an inverse trend can be seen for the share of nucleation mode particles where the  
 442 cumulative PN share of sub-50 nm and sub-23 nm particles decreased from Phase 1 to Phase  
 443 2 and then increases gradually.

444 Figure 4 showed that within Phase 1, which is the formal cold-start period, the PN median  
 445 diameter with different fuels was between 79 to 94 nm. Figure 6 also showed how the median  
 446 diameter changed through different phases as the engine exhaust temperature increased.  
 447 Figure 8 shows that in Phase 1, with different fuels, between 19 to 29% of PN and less than  
 448 0.8% of PM are in the nucleation mode (5-50 nm). Out of that, the share of sub-23 nm was  
 449 between 1 to 9% for PN and less than 0.02% for PM. During cold-start (Phase 1), the low  
 450 temperature of the exhaust pipe can decrease the exhaust gas temperature and within this

451 cooling process, the volatile materials can nucleate homogeneously into particles [66]. The  
452 reason for this is that a decrease in the exhaust gas temperature increases the saturation  
453 vapour pressure and saturation ratio of the volatile materials, which can lead to nucleation  
454 and condensation of volatile materials [67]. It is reported that VOCs during cold-start are  
455 higher than hot-start [68], therefore there is a high chance of nucleation. This is more  
456 significant with biofuel blends owing to their higher VOCs compared to diesel [69].

457 Figure 7 shows that in Phase 2, the particle size distribution graph tends toward higher PN  
458 and also bigger particles when compared to Phase 1. This can be better seen in Figure 6 where  
459 the median diameter of particles increased from Phase 1 to Phase 2. As an example, the PN  
460 median diameter increased from 86 nm to 99 nm with D100. The increase in median diameter  
461 from Phase 1 to Phase 2 was between 7 to 15%. Moving toward bigger particles in Phase 2  
462 can also be seen by comparing the red colour to the blue colour in Figure 7 and in Figure 8  
463 where the cumulative share of PN in the nucleation mode decreased significantly in Phase 2  
464 compared to Phase 1. For example, with D100, the share of nucleation mode particles  
465 decreased from 20% to 12%, with D85C15 the decrease was from 30 to 20%. The share of  
466 sub-23 nm particles also decreased in Phase 2. The reason for this move toward bigger  
467 particles can be due to the injection strategy change within this unsteady warm-up phase in  
468 which the start of injection increased significantly and led to decreased ignition delay  
469 adversely affecting fuel atomisation and premixed combustion. The other variable between  
470 Phases 1 and 2 was the engine temperature, however, this parameter might not be the reason  
471 for the increased diameter size. The observed trend in Figure 6 showed that increasing the  
472 engine temperature can lead to a decrease in the size of particles. The decreasing trend of  
473 median diameter between Phase 2 to Phase 4 in Figure 6 can show that.

474 In Phase 3, particles were smaller than Phase 2, however, they are still bigger than Phase 1  
475 (with most of the fuels). This can be seen in Figure 6 and Figure 7. In this phase, the median  
476 diameter of the particles with different fuels was mostly between 82 to 88 nm (Figure 4). In  
477 this phase, the start of injection stayed constant, however, the engine temperature—  
478 presented by exhaust temperature—was still increasing. Comparing Phase 3 to Phase 2,  
479 Figure 6 shows that the increasing trend of exhaust temperature is associated with a decrease  
480 in median diameter. This can also be seen in Figure 8 where the share of nucleation mode  
481 particles increased compared to Phase 2. For example, with D100, the sub-50 nm particle  
482 share increased from 12 to 18% and from 14 to 17% with D85C15. Also, in this phase, the  
483 share of sub-23 nm particles increased.

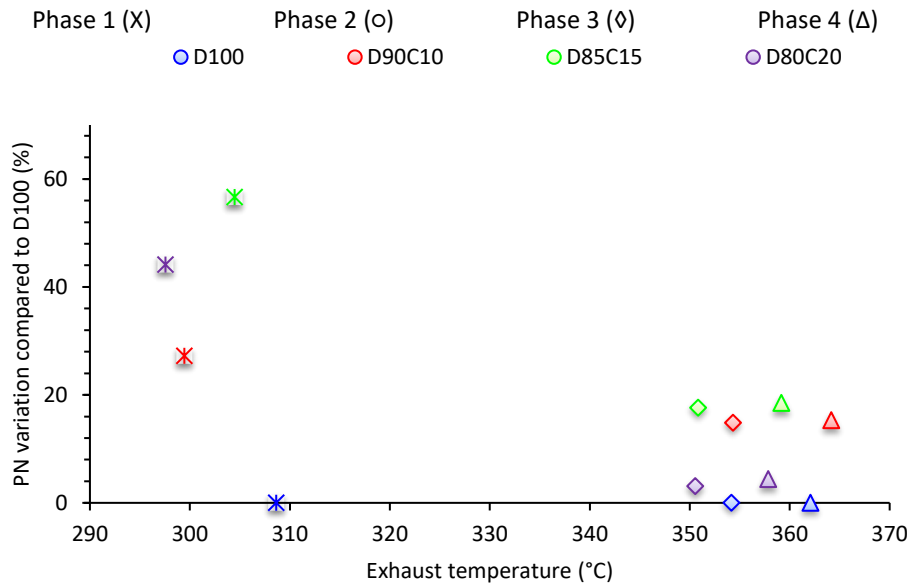
484 Comparing Phase 4 to Phase 3 and Phase 2 shows that the increased exhaust temperature is  
485 associated with a decrease in particle size. This decreasing trend between the median  
486 diameter and exhaust temperature can be seen in Figure 6. It can also be seen in Figure 8 that  
487 the share of nucleation mode particles in Phase 4 was higher than Phase 3. This can be due  
488 to the effect of sub-optimal engine oil temperature. However, the change was small with most  
489 of the fuels. For example, with D80C20, the nucleation mode particles increased from 17 to  
490 18%. Comparing Phase 4 to Phase 1 shows a different trend with different fuels, which means  
491 that the fuel properties are likely to be the driving factor.

### 492 **3.2 Effect of fuel**

493 Figure 3 showed that the PN concentration increased in all of the phases when the fuel blends  
494 were used instead of diesel. For example, using D90C10 increased PN by 27, 36, 15 and 15%  
495 from Phase 1 to 4, respectively. The reason for this can be the higher volatile organic  
496 compounds (VOCs) of biofuels when compared to diesel [69]. It was also observed in Figure 5

497 that compared to D100, these fuels showed less difference between cold-start and hot-  
498 operation. Comparing Phase 3 and 4 to Phase 1, in Figure 5, shows that the PN variation  
499 decreased by increasing the share of biofuel in the blend. For example, with D100, D90C10,  
500 D85C15 and D80C20, PN during Phase 4 was 52, 38, 15 and 10% higher than Phase 1.  
501 However, this can be misleading, and the data can be evaluated from another aspect. Figure  
502 10 shows how the PN concentration changed with different fuels compared to D100. It can  
503 be seen that using D90C10, D85C15 and D80C20, instead of D100, increased the PN  
504 concentration in all of the phases. However, the increase was more significant during cold-  
505 start. For example, in Phase 1, which is cold-start, using these fuels instead of D100 increased  
506 PN between 27 to 57%; while, during hot-operation the increase range was between 4 to 19%.  
507 This is an important observation because using these fuels has more adverse impacts within  
508 the cold-start period, which is an inevitable part of daily driving for most vehicles. This analysis  
509 shows that the evaluation of using such fuels needs to be done not only during hot-operation,  
510 but also cold-start. A reason for the increased PN with the fuel blends during cold-start could  
511 be the higher viscosity of biofuels, which adversely affects fuel atomisation and evaporation  
512 [70]. Another reason could be the increased number of small particles. The higher oxygen  
513 content of biofuels can also result in higher PN. In biofuels, there is more oxygen available in  
514 the center of the diffusion flame (where usually the concentration of HC is higher). This could  
515 result in smaller primary particle diameters and an increase of smaller size particles.

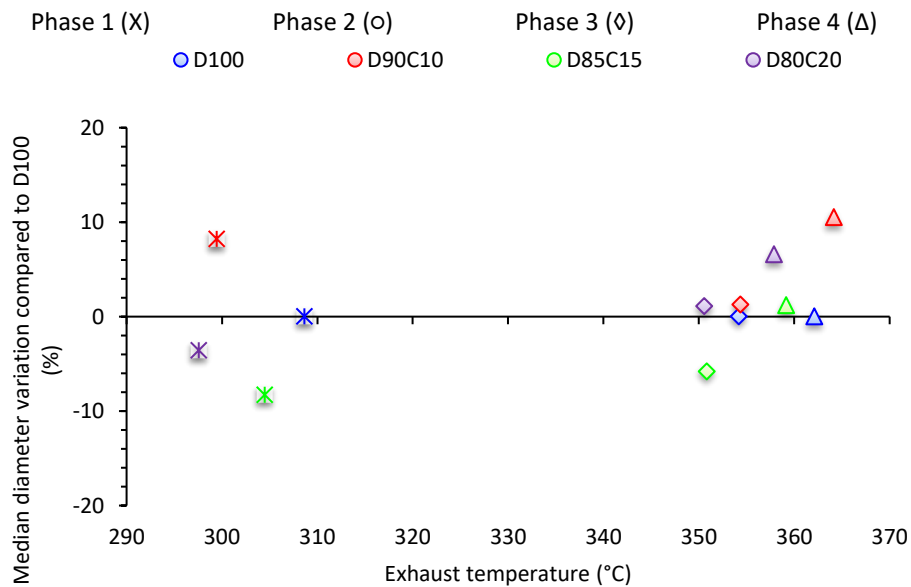
516 The adverse effect of using biofuels can be further highlighted in Figure 11, where the PN  
517 median diameter with these fuels during the first two phases is smaller than D100 (in most of  
518 the cases); while during Phase 4, D100 has the lowest median diameter. This means that these  
519 fuels emit smaller particles during cold-start. This is important as a decrease in particle size  
520 has been shown to be associated with an increase in toxicity [33].



521

522 Figure 10 PN variation compared to D100 vs. exhaust gas temperature at different phases with all of  
 523 the tested fuels

524



525

526 Figure 11 Median diameter variation compared to D100 vs. exhaust gas temperature at different  
 527 phases

528

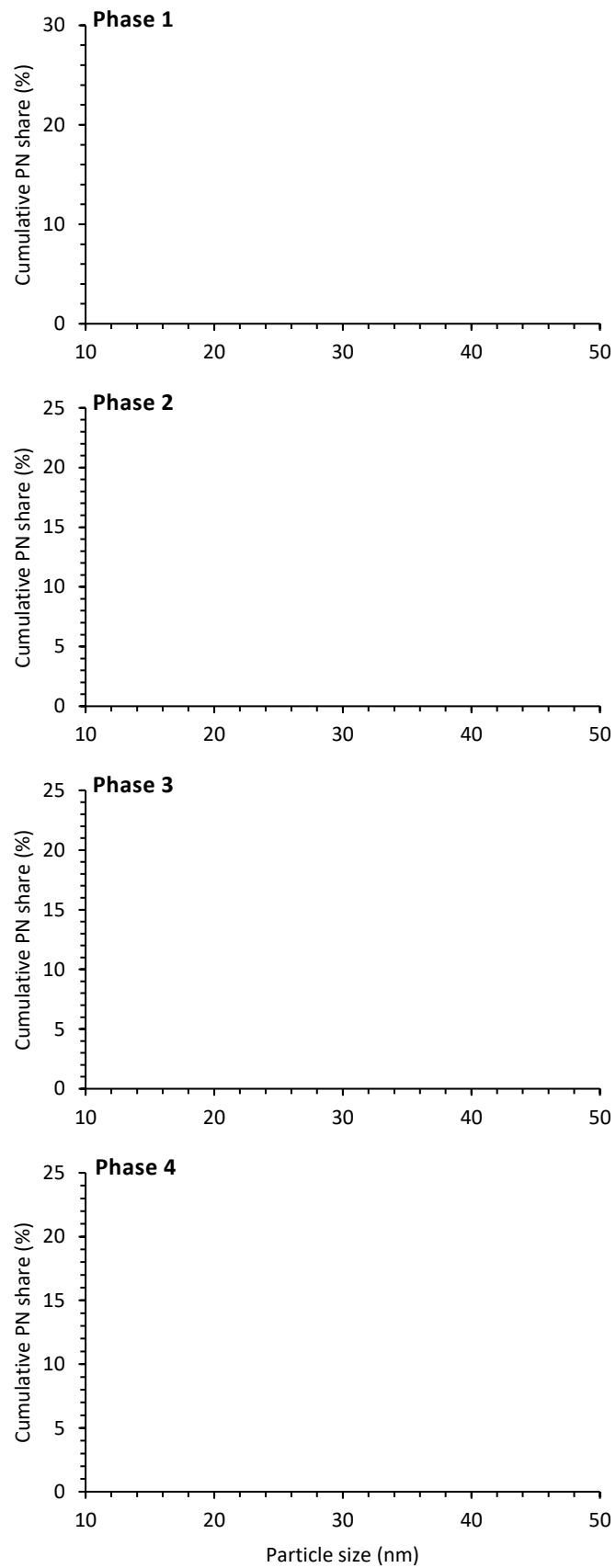
529 The increase in smaller particles is shown in Figure 12 which shows the cumulative share of  
 530 nucleation mode particles at different phases. Figure 12 shows that during cold-start the

531 share of nucleation mode particles increased significantly when D100 was replaced by the  
532 fuel blends. For example, the share of sub-50 nm particles with D100, D90C10, D85C15 and  
533 D80C20 were 20, 20, 29 and 23% in Phase 1, and 12, 12, 20 and 14% in Phase 2, respectively.  
534 A similar trend was also observed for sub-23 nm particles. For example, the share of these  
535 particles in Phase 1 increased from 1 to 9% when D100 was replaced with D85C15.

536 It was mentioned that nucleation mode particles (sub-50 nm) are mainly volatile organic  
537 compounds (VOCs), sulfur compounds, metal compounds and solid carbons [28]. It is known  
538 that biofuels have higher VOCs compared to diesel [69], therefore the higher VOCs of the  
539 tested fuels compared to D100 could be the reason for the increased share of nucleation  
540 mode particles and therefore the total PN. A greater amount of VOCs with biofuel was also  
541 reported by Hedayat et al. [71], which used the same type of engine as this study, under a  
542 stationary cycle.

543

○ D100   ○ D90C10   ○ D85C15   ○ D80C20



544

Figure 12 Cumulative PN share at different phases with all of the tested fuels

### 545 **3.3 Practical implications of this study**

546 Due to the high price and adverse health effects of fossil fuels, there is a focus to increase the  
547 use of biofuels and measures have been in place. However, vehicle emissions are still an issue  
548 and governments and authorities are trying to limit the amount of emission by tightening the  
549 emissions levels from vehicles in the emission regulations. This research is related to the  
550 future emissions regulations (Euro 7) and introduces important knowledge about regulated  
551 and currently-unregulated particulate number emissions during cold-start and engine warm-  
552 up, which is an emerging area in the literature. This study shows that when it comes to very  
553 small particles (which are more toxic), the current market trend (increasing the share of  
554 biofuel) can have a more adverse impact (because of more small particles) within the cold-  
555 start period—which is inevitable in most vehicles’ daily driving schedule. But, even the latest  
556 emission regulations, such as WLTP, only consider particles with a size above 23 nm. Most  
557 cold-start operations occur in residential areas, and this study shows that a significant portion  
558 of emitted particles are smaller than 23 nm during cold-start, and also the current fuel market  
559 leads to an even higher number of these small particles. And the current regulations do not  
560 include a practical enough measure to limit such emissions. Including sub-23 nm particles in  
561 regulations (through PMP) increases the number of particles measured during the  
562 homologation tests, and this might lead many vehicles to fail to comply with the PN limit in  
563 emissions certification tests. However, passing or failing the certification test does not change  
564 the fact that these days many certified vehicles on the street are emitting a huge number of  
565 small particles affecting people’s health and still the emission regulations are unable to stop  
566 them. This study emphasizes the importance of including smaller (sub-23 nm) particles in  
567 future regulations, or even in the new amendments of the current regulations.

#### 568 **4. Conclusions**

569 Using a diesel engine fueled by diesel and biofuels, this research evaluated PN, PN and PM  
570 median diameter, PN and PM size distribution, the share of particles at different sizes  
571 including nucleation mode and sub-23 nm particles. This research divided the engine warm-  
572 up period into four phases of cold-start (Phase 1) to hot-operation (Phase 4) and two  
573 intermediate unsteady warm-up phases which could be counted neither as cold-start (defined  
574 in the regulations) nor as hot-operation.

575 Results showed that for all of the fuels, compared to Phase 1, PN increased by 27-39% in  
576 Phase 2, 11-55% in Phase 3 and 10-52% in Phase 4. In the cold-start phase, between 19 to  
577 29% of the total PN and less than 0.8% of the total PM were related to particles in the  
578 nucleation mode (sub-50 nm). Out of that, the share of sub-23 nm was between 1 to 9% for  
579 PN and less than 0.02% for PM. By using biofuel blends instead of diesel, PN increased  
580 between 27 to 57% during cold-start; while, during hot-operation, the increase in PN ranged  
581 between 4 to 19%. Also, the PN median diameter decreased during the first two phases and  
582 nucleation mode particles increased significantly. For all of the fuels at the different phases,  
583 the PM median diameter was between 173 to 213 nm, while for PN the median diameter was  
584 between 79 to 100 nm. The cumulative share of sub-50 nm particles was 0.3-0.9% of the total  
585 mass, while 11-29% of the total PN. For the sub-30 and sub-23 nm particles, the PM  
586 cumulative share was up to 0.06 and 0.02%; while, their PN cumulative share was 13 and 9%,  
587 respectively. The contribution of particles above 50 nm to PM was significantly high. This was  
588 more significant for the sizes above 100 nm where the share of PN was decreasing. Sub-100  
589 nm particles contributed to 53-67% of PN while only to 8-14% of PM. 92-96% of PN was  
590 related to sub-200 nm, while only 50-66% of the total mass was related to this size range. In  
591 the accumulation mode, the share of PN decreased as the share of PM increased.

592 **5. Acknowledgement**

593 The authors would like to acknowledge the support of Australian Research Council Linkage  
594 Projects funding scheme (project number LP110200158), Prof. Jochen Mueller, Mr. Andrew  
595 Elder and Mr. Noel Hartnett for their assistance.

596

597 **6. References**

- 598 1. Joshi, A., *Review of Vehicle Engine Efficiency and Emissions*. SAE International Journal  
599 of Engines, 2020. 10.4271/2020-01-0352.
- 600 2. Verma, T.N., P. Nashine, P.K. Chaurasiya, U. Rajak, A. Afzal, S. Kumar, D.V. Singh and  
601 A.K. Azad, *The effect of ethanol-methanol-diesel-microalgae blends on performance,*  
602 *combustion and emissions of a direct injection diesel engine*. Sustainable Energy  
603 Technologies and Assessments, 2020. **42**: p. 100851.  
604 <https://doi.org/10.1016/j.seta.2020.100851>.
- 605 3. Sathyamurthy, R., D. Balaji, S. Gorjian, S.J. Muthiya, R. Bharathwaaj, S.  
606 Vasanthaseelan and F.A. Essa, *Performance, combustion and emission characteristics*  
607 *of a DI-CI diesel engine fueled with corn oil methyl ester biodiesel blends*. Sustainable  
608 Energy Technologies and Assessments, 2021. **43**: p. 100981.  
609 <https://doi.org/10.1016/j.seta.2020.100981>.
- 610 4. Abrar, I. and A.N. Bhaskarwar, *Performance and emission characteristics of constant*  
611 *speed diesel engine fueled by surfactant-free microemulsions*. Sustainable Energy  
612 Technologies and Assessments, 2021. **47**: p. 101414.  
613 <https://doi.org/10.1016/j.seta.2021.101414>.
- 614 5. Elkelawy, M., A.E. Kabeel, E.A. El Shenawy, H. Panchal, A. Elbanna, H.A.-E. Bastawissi  
615 and K.K. Sadasivuni, *Experimental investigation on the influences of acetone organic*  
616 *compound additives into the diesel/biodiesel mixture in CI engine*. Sustainable Energy  
617 Technologies and Assessments, 2020. **37**: p. 100614.  
618 <https://doi.org/10.1016/j.seta.2019.100614>.
- 619 6. Nabi, M.N., A. Zare, F.M. Hossain, T.A. Bodisco, Z.D. Ristovski and R.J. Brown, *A*  
620 *parametric study on engine performance and emissions with neat diesel and diesel-*  
621 *butanol blends in the 13-Mode European Stationary Cycle*. Energy Conversion and  
622 Management, 2017. **148**: p. 251-259.  
623 <https://doi.org/10.1016/j.enconman.2017.06.001>.
- 624 7. Verma, T.N., P. Shrivastava, U. Rajak, G. Dwivedi, S. Jain, A. Zare, A.K. Shukla and P.  
625 Verma, *A comprehensive review of the influence of physicochemical properties of*  
626 *biodiesel on combustion characteristics, engine performance and emissions*. Journal  
627 of Traffic and Transportation Engineering (English Edition), 2021. **8**(4): p. 510-533.  
628 <https://doi.org/10.1016/j.jtte.2021.04.006>.
- 629 8. Zare, A., M.N. Nabi, T.A. Bodisco, F.M. Hossain, M.M. Rahman, Z.D. Ristovski and R.J.  
630 Brown, *The effect of triacetin as a fuel additive to waste cooking biodiesel on engine*

- 631 *performance and exhaust emissions*. Fuel, 2016. **182**: p. 640-649.  
632 <https://doi.org/10.1016/j.fuel.2016.06.039>.
- 633 9. Zare, A., R.J. Brown and T. Bodisco, *Ethanol Fumigation and Engine Performance in a*  
634 *Diesel Engine, in Alcohol as an Alternative Fuel for Internal Combustion Engines*.  
635 2021, Springer. p. 191-212.
- 636 10. Nabi, M.N., A. Zare, F.M. Hossain, M.M. Rahman, T.A. Bodisco, Z.D. Ristovski and R.J.  
637 Brown, *Influence of fuel-borne oxygen on European Stationary Cycle: Diesel engine*  
638 *performance and emissions with a special emphasis on particulate and NO emissions*.  
639 Energy Conversion and Management, 2016. **127**: p. 187-198.  
640 <https://doi.org/10.1016/j.enconman.2016.09.010>.
- 641 11. Zare, A., T.A. Bodisco, M.N. Nabi, F.M. Hossain, Z.D. Ristovski and R.J. Brown, *Engine*  
642 *Performance during Transient and Steady-State Operation with Oxygenated Fuels*.  
643 Energy & Fuels, 2017. **31**(7): p. 7510-7522. 10.1021/acs.energyfuels.7b00429.
- 644 12. Nabi, M.N., A. Zare, F.M. Hossain, Z.D. Ristovski and R.J. Brown, *Reductions in diesel*  
645 *emissions including PM and PN emissions with diesel-biodiesel blends*. Journal of  
646 Cleaner Production, 2017. **166**: p. 860-868.  
647 <https://doi.org/10.1016/j.jclepro.2017.08.096>.
- 648 13. Bencheikh, K., A.E. Atabani, S. Shobana, M.N. Mohammed, G. Uğuz, O. Arpa, G.  
649 Kumar, A. Ayanoglu and A. Bokhari, *Fuels properties, characterizations and engine*  
650 *and emission performance analyses of ternary waste cooking oil biodiesel–diesel–*  
651 *propanol blends*. Sustainable Energy Technologies and Assessments, 2019. **35**: p.  
652 321-334. <https://doi.org/10.1016/j.seta.2019.08.007>.
- 653 14. Attia, A.M.A., M. Nour, A.I. El-Seesy and S.A. Nada, *The effect of castor oil methyl*  
654 *ester blending ratio on the environmental and the combustion characteristics of*  
655 *diesel engine under standard testing conditions*. Sustainable Energy Technologies  
656 and Assessments, 2020. **42**: p. 100843. <https://doi.org/10.1016/j.seta.2020.100843>.
- 657 15. Lapuerta, M., O. Armas and J. Rodríguez-Fernández, *Effect of biodiesel fuels on diesel*  
658 *engine emissions*. Progress in Energy and Combustion Science, 2008. **34**(2): p. 198-  
659 223. <https://doi.org/10.1016/j.pecs.2007.07.001>.
- 660 16. de Moraes, A.M., S. de Moraes Hanriot, A. de Oliveira, M.A.M. Justino, O.S. Valente  
661 and J.R. Sodr , *An assessment of fuel consumption and emissions from a diesel power*  
662 *generator converted to operate with ethanol*. Sustainable Energy Technologies and  
663 Assessments, 2019. **35**: p. 291-297. <https://doi.org/10.1016/j.seta.2019.08.005>.
- 664 17. Singh, G., A.P. Singh and A.K. Agarwal, *Experimental investigations of combustion,*  
665 *performance and emission characterization of biodiesel fuelled HCCI engine using*  
666 *external mixture formation technique*. Sustainable Energy Technologies and  
667 Assessments, 2014. **6**: p. 116-128. <https://doi.org/10.1016/j.seta.2014.01.002>.
- 668 18. Giakoumis, E.G., C.D. Rakopoulos, A.M. Dimaratos and D.C. Rakopoulos, *Exhaust*  
669 *emissions of diesel engines operating under transient conditions with biodiesel fuel*  
670 *blends*. Progress in Energy and Combustion Science, 2012. **38**(5): p. 691-715.  
671 <https://doi.org/10.1016/j.pecs.2012.05.002>.
- 672 19. Datta, A. and B.K. Mandal, *A comprehensive review of biodiesel as an alternative fuel*  
673 *for compression ignition engine*. Renewable and Sustainable Energy Reviews, 2016.  
674 **57**: p. 799-821. <https://doi.org/10.1016/j.rser.2015.12.170>.
- 675 20. Nabi, N., A. Zare, M. Hossain, M.M. Rahman, D. Stuart, Z. Ristovski and R. Brown.  
676 *Formulation of new oxygenated fuels and their influence on engine performance and*  
677 *exhaust emissions*. The Combustion Institute Australia and New Zealand Section.

- 678 21. Verma, P., S. Stevanovic, A. Zare, G. Dwivedi, T. Chu Van, M. Davidson, T. Rainey, R.J.  
679 Brown and Z.D. Ristovski, *An overview of the influence of biodiesel, alcohols, and*  
680 *various oxygenated additives on the particulate matter emissions from diesel*  
681 *engines*. *Energies*, 2019. **12**(10): p. 1987
- 682 22. World Health Organization, *Review of evidence on health aspects of air pollution–*  
683 *REVIHAAP Project*. 2013
- 684 23. Vaughan, A., S. Stevanovic, A.P. Banks, A. Zare, M.M. Rahman, R.V. Bowman, K.M.  
685 Fong, Z.D. Ristovski and I.A. Yang, *The cytotoxic, inflammatory and oxidative*  
686 *potential of coconut oil-substituted diesel emissions on bronchial epithelial cells at an*  
687 *air-liquid interface*. *Environmental Science Pollution Research*, 2019. **26**(27): p.  
688 27783-27791
- 689 24. Vaughan, A., S. Stevanovic, M. Rahman, A. Zare, B. Miljevic, Z. Ristovski, R. Bowman,  
690 K. Fong and I. Yang, *N-acetyl cysteine (NAC) intervention attenuates the effects of*  
691 *diesel and biodiesel emission exposure on human bronchial epithelial cells, 16HBE, at*  
692 *air-liquid interface*. *European Respiratory Journal*, 2016
- 693 25. Stevanovic, S., A. Vaughan, F. Hedayat, F. Salimi, M.M. Rahman, A. Zare, R.A. Brown,  
694 R.J. Brown, H. Wang and Z. Zhang, *Oxidative potential of gas phase combustion*  
695 *emissions-An underestimated and potentially harmful component of air pollution*  
696 *from combustion processes*. *Atmospheric environment*, 2017. **158**: p. 227-235
- 697 26. Vaughan, A., S. Stevanovic, A. Zare, M. Rahman, B. Miljevic, Z. Ristovski, R. Bowman,  
698 K. Fong and I. Yang, *Coconut oil substitution in diesel fuel alters human bronchial*  
699 *epithelial cell responses to diesel emission exposure at the air-liquid interface in vitro:*  
700 *to O22*. *Respirology*, 2016. **21**
- 701 27. Vaughan, A., S. Stevanovic, L.E. Morrison, A.M. Pourkhesalian, M.M. Rahman, A.  
702 Zare, B. Miljevic, F. Goh, V. Relan and R. Bowman, *Removal of organic content from*  
703 *diesel exhaust particles alters cellular responses of primary human bronchial*  
704 *epithelial cells cultured at an air-liquid interface*. *Journal of Environmental Analytical*  
705 *Toxicology*, 2015. **5**(5): p. 100316-1
- 706 28. Kittelson, D.B., *Engines and nanoparticles: a review*. *Journal of aerosol science*, 1998.  
707 **29**(5-6): p. 575–588
- 708 29. Delphi Technologies, *Worldwide emissions standards-Passenger cars and light duty*  
709 *vehicles*. Delphi, 2019. <https://www.delphi.com/innovations>.
- 710 30. Chen, L., S. Ding, H. Liu, Y. Lu, Y. Li and A.P. Roskilly, *Comparative study of*  
711 *combustion and emissions of kerosene (RP-3), kerosene-pentanol blends and diesel in*  
712 *a compression ignition engine*. *Applied Energy*, 2017. **203**: p. 91-100
- 713 31. Zare, A., T.A. Bodisco, M.N. Nabi, F.M. Hossain, M.M. Rahman, Z.D. Ristovski and R.J.  
714 Brown, *The influence of oxygenated fuels on transient and steady-state engine*  
715 *emissions*. *Energy*, 2017. **121**: p. 841-853.  
716 <https://doi.org/10.1016/j.energy.2017.01.058>.
- 717 32. Chen, L., X. Hu, J. Wang and Y. Yu, *Impacts of alternative fuels on morphological and*  
718 *nanostructural characteristics of soot emissions from an aviation piston engine*.  
719 *Environmental science & technology*, 2019. **53**(8): p. 4667-4674
- 720 33. Krahl, J., J. Büniger, O. Schröder, A. Munack and G. Knothe, *Exhaust emissions and*  
721 *health effects of particulate matter from agricultural tractors operating on rapeseed*  
722 *oil methyl ester*. *Journal of the American Oil Chemists' Society*, 2002. **79**(7): p. 717-  
723 724

- 724 34. Giechaskiel, B., T. Lähde, S. Gandi, S. Keller, P. Kreutziger and A. Mamakos,  
725 *Assessment of 10-nm Particle Number (PN) Portable Emissions Measurement*  
726 *Systems (PEMS) for Future Regulations*. International Journal of Environmental  
727 Research and Public Health, 2020. **17**(11). 10.3390/ijerph17113878.
- 728 35. Giechaskiel, B., *Effect of Sampling Conditions on the Sub-23 nm Nonvolatile Particle*  
729 *Emissions Measurements of a Moped*. Applied Sciences, 2019. **9**(15).  
730 10.3390/app9153112.
- 731 36. Giechaskiel, B., T. Lähde, A.D. Melas, V. Valverde and M. Clairotte, *Uncertainty of*  
732 *laboratory and portable solid particle number systems for regulatory measurements*  
733 *of vehicle emissions*. Environmental Research, 2021. **197**: p. 111068.  
734 <https://doi.org/10.1016/j.envres.2021.111068>.
- 735 37. Andersson, J., A. Mamakos, Z.C. Samaras, Z. Toumasatos, A. Kontses, L.D.  
736 Ntziachristos, A. Bergmann, S. Hausberger, L. Landl, M. Bainschab, J. Keskinen and C.  
737 Haisch, *Measuring Automotive Exhaust Particles Down to 10 nm*. SAE International  
738 Journal of Advances and Current Practices in Mobility, 2020. **3**(1): p. 539-550.  
739 <https://doi.org/10.4271/2020-01-2209>.
- 740 38. Leach, F., A. Lewis, S. Akehurst, J. Turner and D. Richardson, *Sub-23 nm particulate*  
741 *emissions from a highly boosted GDI engine*. SAE Technical Paper, 2019. 0148-7191.
- 742 39. Lodi, F., A. Zare, P. Arora, S. Stevanovic, P. Verma, M. Jafari, Z. Ristovski, R. Brown  
743 and T. Bodisco, *Characteristics of Particle Number and Particle Mass Emissions of a*  
744 *Diesel Engine during Cold-, Warm-, and Hot-Start Operation*. SAE Technical Paper,  
745 2021. <https://doi.org/10.4271/2021-01-5061>.
- 746 40. Reiter, M.S. and K.M. Kockelman, *The problem of cold starts: A closer look at mobile*  
747 *source emissions levels*. Transportation Research Part D: Transport and Environment,  
748 2016. **43**: p. 123-132
- 749 41. André, M., *In actual use car testing: 70,000 kilometers and 10,000 trips by 55 French*  
750 *cars under real conditions*. SAE transactions, 1991: p. 65-72
- 751 42. Zare, A., S. Stevanovic, M. Jafari, P. Verma, M. Babaie, L. Yang, M.M. Rahman, Z.D.  
752 Ristovski, R.J. Brown and T.A. Bodisco, *Analysis of cold-start NO<sub>2</sub> and NO<sub>x</sub> emissions,*  
753 *and the NO<sub>2</sub>/NO<sub>x</sub> ratio in a diesel engine powered with different diesel-biodiesel*  
754 *blends*. Environmental Pollution, 2021. **290**: p. 118052.  
755 <https://doi.org/10.1016/j.envpol.2021.118052>.
- 756 43. Shi, Z., C.-f. Lee, H. Wu, Y. Wu, L. Zhang and F. Liu, *Optical diagnostics of low-*  
757 *temperature ignition and combustion characteristics of diesel/kerosene blends under*  
758 *cold-start conditions*. Applied Energy, 2019. **251**: p. 113307.  
759 <https://doi.org/10.1016/j.apenergy.2019.113307>.
- 760 44. Lodi, F., A. Zare, P. Arora, S. Stevanovic, M. Jafari, Z. Ristovski, R.J. Brown and T.  
761 Bodisco, *Combustion Analysis of a Diesel Engine during Warm up at Different Coolant*  
762 *and Lubricating Oil Temperatures*. Energies, 2020. **13**(15): p. 3931
- 763 45. Verma, P., M. Jafari, A. Zare, E. Pickering, Y. Guo, C.G. Osuagwu, S. Stevanovic, R.  
764 Brown and Z. Ristovski, *Soot particle morphology and nanostructure with oxygenated*  
765 *fuels: A comparative study into cold-start and hot-start operation*. Environmental  
766 Pollution, 2021. **275**: p. 116592. <https://doi.org/10.1016/j.envpol.2021.116592>.
- 767 46. Zare, A., T.A. Bodisco, M.N. Nabi, F.M. Hossain, Z.D. Ristovski and R.J. Brown, *A*  
768 *comparative investigation into cold-start and hot-start operation of diesel engine*  
769 *performance with oxygenated fuels during transient and steady-state operation*.  
770 Fuel, 2018. **228**: p. 390-404. <https://doi.org/10.1016/j.fuel.2018.05.004>.

- 771 47. Zare, A., M.N. Nabi, T.A. Bodisco, F.M. Hossain, M.M. Rahman, T. Chu Van, Z.D.  
772 Ristovski and R.J. Brown, *Diesel engine emissions with oxygenated fuels: A*  
773 *comparative study into cold-start and hot-start operation*. Journal of Cleaner  
774 Production, 2017. **162**: p. 997-1008. <https://doi.org/10.1016/j.jclepro.2017.06.052>.
- 775 48. Lodi, F., A. Zare, P. Arora, S. Stevanovic, M. Jafari, Z. Ristovski, R.J. Brown and T.  
776 Bodisco, *Engine Performance and Emissions Analysis in a Cold, Intermediate and Hot*  
777 *Start Diesel Engine*. Applied Sciences, 2020. **10**(11): p. 3839
- 778 49. Nam, E., *Analysis of particulate matter emissions from light-duty gasoline vehicles in*  
779 *Kansas City*. 2008: US Environmental Protection Agency.
- 780 50. Lee, D.-W., J. Johnson, J. Lv, K. Novak and J. Zietsman, *Comparisons between*  
781 *vehicular emissions from real-world in-use testing and EPA moves estimation*. Texas  
782 Transportation Institute, 2012.
- 783 51. Roberts, A., R. Brooks and P. Shipway, *Internal combustion engine cold-start*  
784 *efficiency: A review of the problem, causes and potential solutions*. Energy  
785 Conversion and Management, 2014. **82**: p. 327-350
- 786 52. Zare, A., T.A. Bodisco, P. Verma, M. Jafari, M. Babaie, L. Yang, M.M. Rahman, A.  
787 Banks, Z.D. Ristovski and R.J. Brown, *Emissions and performance with diesel and*  
788 *waste lubricating oil: A fundamental study into cold start operation with a special*  
789 *focus on particle number size distribution*. Energy Conversion and Management,  
790 2020. **209**: p. 112604
- 791 53. Bodisco, T. and R.J. Brown, *Inter-cycle variability of in-cylinder pressure parameters*  
792 *in an ethanol fumigated common rail diesel engine*. Energy, 2013. **52**: p. 55-65
- 793 54. Bodisco, T., P. Tröndle and R.J. Brown, *Inter-cycle variability of ignition delay in an*  
794 *ethanol fumigated common rail diesel engine*. Energy, 2015. **84**: p. 186-195
- 795 55. Su, S., T. Lv, Y. Lai, J. Mu, Y. Ge and B. Giechaskiel, *Particulate emissions of heavy*  
796 *duty diesel engines measured from the tailpipe and the dilution tunnel*. Journal of  
797 Aerosol Science, 2021. **156**: p. 105799.  
798 <https://doi.org/10.1016/j.jaerosci.2021.105799>.
- 799 56. Giechaskiel, B., A.D. Melas, T. Lähde and G. Martini, *Non-Volatile Particle Number*  
800 *Emission Measurements with Catalytic Strippers: A Review*. Vehicles, 2020. **2**(2).  
801 10.3390/vehicles2020019.
- 802 57. TSI, *Aerosol Instrument Manager® Software for Scanning Mobility Particle Sizer™*  
803 *(SMPS™) Spectrometer*. 2010, TSI. p. 71.
- 804 58. Giakoumis, E.G., C.D. Rakopoulos and D.C. Rakopoulos, *Assessment of NOx Emissions*  
805 *during Transient Diesel Engine Operation with Biodiesel Blends*. Journal of Energy  
806 Engineering 2014. **140**(3): p. A4014004. doi:10.1061/(ASCE)EY.1943-7897.0000136.
- 807 59. Van, T.C., A. Zare, M. Jafari, T.A. Bodisco, N. Surawski, P. Verma, K. Suara, Z.  
808 Ristovski, T. Rainey and S. Stevanovic, *Effect of cold start on engine performance and*  
809 *emissions from diesel engines using IMO-Compliant distillate fuels*. Environmental  
810 Pollution, 2019. **255**: p. 113260
- 811 60. Mitchell, B.J., A. Zare, T.A. Bodisco, M.N. Nabi, F.M. Hossain, Z.D. Ristovski and R.J.  
812 Brown, *Engine blow-by with oxygenated fuels: A comparative study into cold and hot*  
813 *start operation*. Energy, 2017. **140**: p. 612-624
- 814 61. Zare, A., T.A. Bodisco, M. Jafari, P. Verma, L. Yang, M. Babaie, M.M. Rahman, A.  
815 Banks, Z.D. Ristovski, R.J. Brown and S. Stevanovic, *Cold-start NOx emissions: Diesel*  
816 *and waste lubricating oil as a fuel additive*. Fuel, 2021. **286**: p. 119430.  
817 <https://doi.org/10.1016/j.fuel.2020.119430>.

- 818 62. Chien, S.-M., Y.-J. Huang, S.-C. Chuang and H.-H. Yang, *Effects of biodiesel blending*  
819 *on particulate and polycyclic aromatic hydrocarbon emissions in*  
820 *nano/ultrafine/fine/coarse ranges from diesel engine*. *Aerosol and Air Quality*  
821 *Research*, 2016. **9**(1): p. 18-31
- 822 63. Jafari, M., P. Verma, T.A. Bodisco, A. Zare, N.C. Surawski, P. Borghesani, S.  
823 Stevanovic, Y. Guo, J. Alroe, C. Osuagwu, A. Milic, B. Miljevic, Z.D. Ristovski and R.J.  
824 Brown, *Multivariate analysis of performance and emission parameters in a diesel*  
825 *engine using biodiesel and oxygenated additive*. *Energy Conversion and*  
826 *Management*, 2019. **201**: p. 112183.  
827 <https://doi.org/10.1016/j.enconman.2019.112183>.
- 828 64. Yusuf, A.A. and F.L. Inambao, *Effect of cold start emissions from gasoline-fueled*  
829 *engines of light-duty vehicles at low and high ambient temperatures: Recent trends*.  
830 *Case Studies in Thermal Engineering*, 2019. **14**: p. 100417.  
831 <https://doi.org/10.1016/j.csite.2019.100417>.
- 832 65. Kittelson, D.B., W.F. Watts, J.P. Johnson, C. Thorne, C. Higham, M. Payne, S. Goodier,  
833 C. Warrens, H. Preston and U. Zink, *Effect of fuel and lube oil sulfur on the*  
834 *performance of a diesel exhaust gas continuously regenerating trap*. *Environmental*  
835 *science & technology*, 2008. **42**(24): p. 9276-9282
- 836 66. Ning, Z., C.S. Cheung and S.X. Liu, *Experimental investigation of the effect of exhaust*  
837 *gas cooling on diesel particulate*. *Journal of Aerosol Science*, 2004. **35**(3): p. 333-345
- 838 67. Kasper, M., *Sampling and measurement of nanoparticle emissions for type approval*  
839 *and field control*. SAE Technical Paper, 2005. 0148-7191.
- 840 68. Tsai, J.-H., S.-Y. Chang and H.-L. Chiang, *Volatile organic compounds from the exhaust*  
841 *of light-duty diesel vehicles*. *Atmospheric environment*, 2012. **61**: p. 499-506
- 842 69. Pourkhesalian, A.M., S. Stevanovic, F. Salimi, M.M. Rahman, H. Wang, P.X. Pham, S.E.  
843 Bottle, A.R. Masri, R.J. Brown and Z.D. Ristovski, *Influence of fuel molecular structure*  
844 *on the volatility and oxidative potential of biodiesel particulate matter*.  
845 *Environmental science & technology*, 2014. **48**(21): p. 12577-12585
- 846 70. Armas, O., J.J. Hernández and M.D. Cárdenas, *Reduction of diesel smoke opacity from*  
847 *vegetable oil methyl esters during transient operation*. *Fuel*, 2006. **85**(17-18): p.  
848 2427-2438
- 849 71. Hedayat, F., S. Stevanovic, A. Milic, B. Miljevic, M.N. Nabi, A. Zare, S.E. Bottle, R.J.  
850 Brown and Z.D. Ristovski, *Influence of oxygen content of the certain types of*  
851 *biodiesels on particulate oxidative potential*. *Science of The Total Environment*, 2016.  
852 **545-546**: p. 381-388. <https://doi.org/10.1016/j.scitotenv.2015.12.036>.

853

854

855

856

857 **7. Appendix A**

858 Table A1 shows the accuracy of the measuring instruments.

859 Table A1 Instrument accuracy

<b>Instrument</b>	<b>Accuracy</b>
Kistler 6053CC60 piezoelectric transducer	≈ -20 pC/bar
Kistler type 2614	0.5 crank angle degrees
CAI-600 NDIR CO <sub>2</sub> analyser	Linearity > 0.5% and repeatability > 1% of full scale
SABLE CA-10 Carbon CO <sub>2</sub> gas analyser	1% of reading within the range of 0-10%
Dynamometer	±0.5%

860

861 Table A2 shows the statistical analysis of the test repeatability for cold-start and warm-start  
862 tests with diesel using average and coefficient of variation (CoV) of engine speed and torque.

863 As can be seen, the difference between the tests is indicating the repeatability of the  
864 experiment. In addition to these two important parameters, Table A3 shows the CO<sub>2</sub>  
865 repeatability. This experimental study used a non-dispersive infrared CAI-600 CO<sub>2</sub> gas  
866 analyser which is a piece of high-tech quality equipment in the market used by different car  
867 industries and research groups to check the CO<sub>2</sub> emission and confirm the test repeatability.

868 It is worth to mention that using a correlation car/engine and measuring CO<sub>2</sub> in the repeated  
869 tests and then calculating the variation between the correlation tests is a very common and  
870 trustworthy method of uncertainty measurement and test repeatability check in emissions  
871 laboratories of the automotive industries.

872

873

874

875 Table A2 Test repeatability: statistical analysis

		Engine speed (rpm)		Engine torque (Nm)	
		Mean	CoV (%)	Mean	CoV (%)
Warm-start	Test I	1499.49	0.14	242.02	1.00
	Test II	1498.94	0.15	238.28	1.34
	Difference		0.04%		1.5%
Cold-start	Test I	1499.19	0.13	227.20	5.42
	Test II	1498.87	0.15	225.28	3.74
	Difference		0.02%		0.82%

876

877 Table A3 Test repeatability: CO<sub>2</sub> correlation test

		Mean	CoV (%)
Warm-start	Test I	6.64	0.36
	Test II	6.47	0.51
	Difference		0.17%
Cold-start	Test I	6.51	2.27
	Test II	6.36	0.97
	Difference		0.12%

878